Journal of
Environmental Analytical Chemistry
ISSN: 2161-0525

Ebelegi et al., J Environ Anal Chem 2019, 6:2

Research Article Open Access

Facile Uptake of Cadmium (II) from Aqueous Solution Using Polyamidoamine Functionalized Silica

Augustus Newton Ebelegi, Jackson Godwin, Nimibofa Ayawei* and Donbebe Wankasi

Department of Chemical Sciences, Niger Delta University, Bayelsa State, Nigeria

Abstract

An amine terminated G 5.0 Polyamidoamine dendrimer was functionalized with Succinic anhydride and immobilized on chromatography grade silica gel to produce a functionalized dendrimer-silica composite (G-5-PAMAM-SGA). The composite was characterized using Fourier Transform-Infra Red spectroscopy, Brunauer Emmett and Teller surface area analysis, Thermogravimetric Analysis, Zeta Potential, and Scanning Electron Microscopy. Adsorption properties of the synthesized composite were studied by batch adsorption method using Cd (II) as adsorbate. The sorption process was analyzed using 6 different isotherm models (Langmuir, Freundlich, Harkins-Jura, Sips, Jossens and Baudu).

The experimental data were best fitted into Jossens isotherm model (R^2=0.981) the order of fitting for the models is Jossens>Baudu>Harkins-Jura>Sips>Freundlich>Langmuir. The maximum adsorption capacity of G-5-PAMAM-SGA for Cd (II) was 123.4 mg g^{-1} and the system was influenced by temperature, initial concentration and pH. Analysis of sorption kinetics reveals that the data fitted better to the pseudo-second-order model than any other kinetic model, signifying that the sorption process involved is chemisorption. Sticking probability (S^*=0.9999), suggesting a mixture of chemisorption and physisorption (coordination adsorption). Gibbs free energy of adsorption at 293,303 and 313 K were all negative thus sorption was spontaneous and favorable.

Keywords: Polyamidoamine; Succinic anhydride; Isotherm; Chemisorption; Adsorption; Dendrimer; Pseudo-Second-order kinetic model; Harkins-Jura; Baudu

Introduction

The removal of heavy metal ions from industrial effluents is among the worst environmental challenges facing the world today. Heavy metals are chemical elements with a specific gravity that is at least 5 times the specific gravity of water. They are normally challenging environmental pollutants, with renowned toxic effects on living systems [1].

Heavy metals are really hazardous because they are persistent and could remain in the environment long after the original source of pollution is done away with [2].

The mobility of heavy metal ions in ground-water systems is slowed down by reactions that cause metal ions to adsorb or precipitate making them have a propensity to be associated with the solid phase and this usually prevents them from dissolving. While various heavy metal ions undergo similar reactions in a number of aspects, the extent and character of these reactions vary under particular conditions. The uptake of heavy metal ions by plants and subsequent accumulation along the food chain remains a potential threat to human health [3].

Cadmium is a heavy metal with atomic weight 112.4 g/mol it occurs naturally in zinc and lead ores, sedimentary rocks and phosphate fertilizers too [4,5]. Cadmium has been used in the production of alloys, pigments and batteries thus it poses considerable environmental and occupational health concern [6].

Some major sources of widespread cadmium distribution into the environment are: industrial applications, use of phosphate fertilizers in agriculture and sewage sludge. It can also be dispersed via natural emissions and bioaccumulation processes that take place in some plants, mammals and even filter feeder organisms like crustaceans and mulloscs [7]. Other prominent routes for human exposure to cadmium are inhalation of cigarette smoke and ingestion of cadmium infested food and water. Studies have shown that cadmium is very toxic to humans even at very low concentrations because it causes damage to the human body cells through the generation of Reactive Oxygen Species (ROS) that cause single-strand DNA damage which interrupts the synthesis of nucleic acids and proteins [8-10]. Studies have also shown that heightened cadmium intake can cause gastrointestinal tract erosion, pulmonary, hepatic/renal injury and obstructive lung disease [11].

Silica gel, a non-toxic and chemically inert compound composed of amorphous silicon dioxide is used in water purification studies amongst other uses due to its high surface area (800 square meters per gram) arising from the micro-porous structures of interlocking cavities [12,13].

Methods for treating industrial wastewater containing heavy metals often involve processes of toxicity reduction in order to meet technology-based treatment [14]. Some of such heavy metal treatment techniques include chemical precipitation, ion exchange, coagulation/flocculation, ultra-filtration, electrochemical treatment, electrodialysis and adsorption. Adsorption is a well-known, uncomplicated, reasonably priced and proficient means of eradicating heavy metal ions from waste-water using a range of adsorbents such as Bentonite, Fly Ash, Layered Double Hydroxides, Metal Organic Frameworks and many other carbon-based materials [15].

In this study Generation-5 Polyamidoamine dendrimer was

***Corresponding author:** Nimibofa Ayawei, Department of Chemical Sciences, Niger Delta University, Bayelsa State, Nigeria, Tel: +2348034678567; E-mail: ayawei4acad@gmail.com

Received July 16, 2019; **Accepted** August 28, 2019; **Published** September 06, 2019

Citation: Ebelegi AN, Godwin J, Ayawei N, Wankasi D (2019) Facile Uptake of Cadmium (II) from Aqueous Solution Using Polyamidoamine Functionalized Silica. J Environ Anal Chem 6: 258.

functionalized with Succinic anhydride and subsequently immobilized on chromatographic grade silica gel to produce a dendrimer-silica gel composite that was characterized in order to reveal its physicochemical properties. The prepared adsorbent was then tested for its adsorption of Cadmium (II) ions in aqueous solution under optimized reaction conditions of contact time, pH, initial concentration and temperature.

Materials and Methods

Synthesis of G-3 PAMAM functionalized silica

All chemicals used for this study were of Analytical grade. G-5 polyamidoamine (PAMAM) dendrimers with ethylenediamine core, succinic anhydride, cadmium nitrate salt (3-aminopropyl) triethoxysilane (APTES) and chromatographic grade silica gel (particle size-240-425 mesh, pore size-15 nm, pH-7, pore volume-1.15 cm^3/g) were obtained from Sigma Aldrich, South Africa. While N-(3-dimethylaminopropyl-N'-ethylcarbodiimide hydrochloride was procured from Thermo fisher scientific, Belgium.

Grafting APTES on silica

APTES (3-aminopropyl) triethoxysilane) was grafted on silica gel in accordance with a procedure used by Acres et al. [16]. One of the precursor materials silica gel (30 g) was oven dried at 130°C for two hours; by this silica gel crystals were successfully activated. The activated silica gel was then refluxed at 115°C for six hours in a 10% APTES/anhydrous toluene mixture. The resultant product obtained is the amino functionalized silica gel which was subsequently separated from the solution by centrifugation at 4000 rpm for 10 min. The amino functionalized silica gel was washed using water and ethanol alternatively in order to remove excess reagents. The very last wash was done with ethanol after which the product was oven dried at 110°C for one hour.

Functionalization of G-5-PAMAM dendrimer

Another precursor material, Succinic acid terminated generation-5 PAMAM dendrimers was prepared using the method of Shi et al. [17]. Thus, succinic acid terminated generation-5 PAMAM dendrimer was prepared by dissolving about 3.7 mL of G-5-PAMAM dendrimer and 3.1 g succinic anhydride in separate 50 mL volumes of Dimethyl Sulfoxide (DMSO). Both solutions were then transferred into a round bottom flask and refluxed at 80°C for 12 h and dialyzed with deionized water over 3 d (the deionized water was replaced every 6 h). The succinic acid terminated generation-5 PAMAM was withdrawn from the dialysis setup by means of a micropipette and stored for further use.

Coupling functionalized dendrimer unto APTES grafted silica

The final product G-5-PAMAM was prepared using the method of Jiang et al. [18], in which the two precursor materials; silica gel grafted with APTES (20 g) and succinic acid terminated generation-5 PAMAM dendrimer (20 mL) were added into 250 mL round bottom flask containing 75 mL methanol. A coupling agent N-(3-dimethylaminopropyl-N'-ethylcarbodiimide hydrochloride (EDC) (≈5 mg) was added to the flask and the entire mixture was refluxed at 90°C for twelve hours [19]. The final product was separated from excess reagent by centrifugation at 4000 rpm for about 10 min, washed three times with ethanol and oven dried at 110°C for one hour. The final product is the G-5-PAMAM functionalized silica composite (G-5-PAMAM-SGA).

Characterization of the adsorbent

The G-5-PAMAM-SGA and pristine silica were characterized using Fourier Transform Infrared (FTIR) spectrometer in order to determine the associated functional groups using (Spectrum Two, Perkin Elmer Instruments, USA), determination of surface area and porosity was done using Micromeritics TRISTAR II 3020 analyzer (Micromeritics Instrument Corporation, USA). A Zeiss Auriga Field Emission Scanning Electron Microscope (SEM) was used for determination of the adsorbent's surface morphology while thermal stabilities of both materials were determined using thermo-gravimetric analyzer (Perkin-Elmer TGA 4000 by Perkin Elmer Instruments, USA).

Adsorption study

Cadmium nitrate salt was used in the preparation of the stock solution (1000 g/L), after which working solutions were prepared from the stock by serial dilution. Batch adsorption of Cd (II) ions was carried out using G-5-PAMAM-SGA as adsorbent in order to determine the effects of contact time, concentration, pH and temperature. The adsorption procedure was performed as follows; 20 mL of adsorbate solution (specific concentrations) was added to 20 mg of adsorbent material. The adsorbent/adsorbate mixture was then agitated by means of an orbital shaker operating at 200 rpm.

Desorption study

Desorption study was done using 20 mg of previously used adsorbent. Cd (II) ions that were initially adsorbed were desorbed by shaking in 20 mL 0.5 M nitric acid at 220 rpm for duration of 10 min. The plastic centrifuge bottles were removed from the shaker and placed on a centrifuging machine operated at 3500 rpm for 10 min. The amount of Cd (II) ion left in the solution was determined using Atomic Adsorption Spectrometry. The adsorbent was washed twice with dilute nitric acid (0.5 M) and lastly with ultra-pure water before the second round of re-use test (second cycle). The re-use test was carried out for three cycles.

Data management

The adsorption capacity (q_e) and removal capacity (R%) of Cd(II) ions by G-PAMAM-SGA were calculated using the following equations:

$$q_e=[(C_0-C_e)V]/M \quad \ldots\ldots\ldots\ldots \quad (1)$$

$$R(\%)=[(C_0-C_e)/C_0] \times 100 \quad \ldots\ldots\ldots\ldots \quad (2)$$

Where C_0 and C_e (mg/L) are the initial and equilibrium concentrations of Cd(II) ions in solution, V, is the volume of adsorbate solution used (mL) while M, is the mass (g) of adsorbent used for the experiment.

Three kinetics isotherm models Pseudo-First Order (PFO) [20] (Eqn 3), Pseudo-Second Order (PSO) (Eqn 4) kinetics models, and the Weber-Morris [21] intraparticle diffusion (IPD) (Eqn 5)] were used in describing the effect of time data.

$$q_t = q_e(1-e^{-k_1 t}) \quad \ldots\ldots\ldots \quad (3)$$

$$q_t = \frac{q_e^2 k_2 t}{1+q_e k_2 t} \quad \ldots\ldots\ldots \quad (4)$$

$$q_e = k_{IPD} t^{1/2} + C \quad \ldots\ldots\ldots \quad (5)$$

The symbols q_e and q_t are the amounts of Cd(II) adsorbed (mg/g) on the adsorbent (G-5-PAMAM-SGA) at equilibrium and time t, respectively; and k_1 (min^{-1}), k_2 (g/g/min) and k_{IPD} ($g/gmin^{1/2}$) are the rate constants of the PFO, PSO and IPD, respectively; while C (mg/g)

is the amount of Cd(II) adsorbed on the adsorbent surfaces. Model parameters were generated from the KyPlot software.

Equilibrium data at 294 K were calculated using Langmuir (Eqn 4), Freundlich (Eqn 5), Harkins-Jura (Eqn 6), Jossens (Eqn 7), Sips (Eqn 8) and Baudu (Eqn 9). Langmuir, Freundlich and Harkins-Jura equations can be written in the following linear forms [22].

$$\frac{C_e}{q_e} = \frac{1}{q_m K_e} + \frac{C_e}{q_m} \quad (4)$$

Where Ce=concentration of adsorbate at equilibrium (mg g^{-1})

K_L=Langmuir constant related to adsorption capacity (mg g^{-1})

Log q_e=log K_F+1/nlog C_e

Where K_f=Adsorption capacity (L/mg)

1/n=Adsorption intensity, it also indicates the relative distribution of the energy and the heterogeneity of the adsorbent sites.

$$\frac{1}{q_e^2} = \frac{B}{A} - \left(\frac{1}{A}\right)\log C_e \quad (5)$$

Where B and A are Harkins-Jura constants that can be obtained from plotting $1/qe^2$ vs log C_e.

The non-linear forms of Jossens, Sips and Baudu equations are given as follows [22]

$C_e = q_e/H \exp(Fq_e^P)$ …… (7)

Where H=Jossens isotherm constant (it corresponds to Henry's constant), P=Jossens isotherm constant, it is characteristic of the adsorbent irrespective of temperature and the nature of adsorbents. F=Jossens isotherm constant.

$$q_e = \frac{K_s C_e^{\beta s}}{1 - a_s C_e^{\beta s}} \quad (8)$$

Where K_S=Sips isotherm model constant (L g^{-1})

β_s=Sips isotherm exponent

a_s=Sips isotherm model constant (Lg^{-1})

$$q_e = \frac{q_m b_o C_e^{1+x+y}}{1 + b_o C_e^{1+x}} \quad (9)$$

Where q_m=Baudu maximum adsorption capacity (mg g^{-1})

b_o=Equilibrium constant

x=Baudu parameter

y=Baudu parameter

Thermodynamic parameters such enthalpy change, and entropy change were calculated using Vant Hoff (equation 10) and Gibbs free energy of adsorption was evaluated using equation 11.

$\ln K = \Delta S/R - \Delta H/RT$ …….. (10)

$\Delta G^* = \Delta H^* - T\Delta S^*$ …… (11)

Where T is temperature (K) and R is the ideal gas constant (8.314 $J.mol^{-1}K^{-1}$).

The linear form of the modified Arrhenius expression was applied to the experimental data to evaluate the activation energy (E_a) and sticking probability S^* as shown in equation 12.

$ln\,(1-\theta) = ln\,S^* + E_a/RT$ ……12

Where θ is the degree of surface coverage.

Results and Discussion

Physical and chemical characterizations

Results of the physical and chemical characterization of G-5-PAMAM-SGA confirmed the successful synthesis of the composite (G-5-PAMAM-SGA) are shown in Figure 1a, the point of zero charge (pH_{pzc}) was 2.9. Thus, the surface of G-5-PAMAM-SGA becomes predominantly negative above this pH value. The N_2 adsorption/desorption isotherm (not shown) were the classical type IV isotherm, which is an indication for a mesoporous material; the BET surface area was 4.0 m^2/g with a relatively large pore width of 22.4 nm which is higher than that for many reported silica-based adsorbents [23]. This large pore width has more space for large contaminant molecules to be removed from solution via pore filling [24]. The FTIR spectra of the pristine Silica gel and G-5-PAMAM-SGA are shown in Figure 1b. The peaks observed at 1060 and 1800 cm^{-1} are characteristic peaks for silanol groups [23]. While the peak at 1630 cm^{-1} is attributable to the newly introduced amide group.

The TGA spectra (Figure 1c) showed two major thermal transitions for the pristine Silica gel and G-5-PAMAM-SGA as temperature was gradually increased from 40 to 900°C. The initial transition was observed below 150°C for both materials, this was ascribed to loss of physisorbed water molecules within the layer bed of the basic silica material [23]. The higher weight loss exhibited by G-5-PAMAM-SGA at lower temperatures confirms the presence of APTES and PAMAM dendrimers groups which were more labile than the backbone silica material. Thus, the weight loss at this second thermal transition could be attributed to the endothermic decompositions of surface hydroxyl groups on the pristine silica gel and G-5-PAMAM-SGA as well as the APTES and PAMAM groups. The pre and post-adsorption G-5-PAMAM-SGA SEM images are shown in Figures 1d-1e. The Figure 1e showed shinny agglomerated surfaces due to the presence of the adsorbed Cd(II) cations.

Adsorption rate and Kinetics of Cd(II) uptake by G-5-PAMAM-SGA

The adsorption of Cd(II) ions by G-5-PAMAM-SGA as a function of time is illustrated in Figure 2. From the figure it can be deduced that adsorption rate was quite fast initially owing to availability of many vacant surface adsorption sites (10-90 min) but at about 180 min adsorption-desorption rate was stabilized, after which no significant uptake of Cd(II) ions was observed because most adsorption sites were already occupied by Cd(II) ions, thus equilibrium is attained. The kinetics of Cd(II) adsorption by the adsorbent was also obtained from the time data, this is shown in Table 1. Results from Table 1 reveal that the pseudo-second-order kinetic model had the best fitting correlation coefficient (r^2=0.999) indicating that the sorption process could be mainly controlled by chemical interactions between Cd(II) ions and active functional groups on the surface of G-5-PAMAM-SGA. A related result was reported for the adsorption of Cd(II) ions from aqueous solutions using nano zero valent Iron particles [24].

Intra Particle diffusion kinetic model constant, C (mg/g) gave a clue to the pattern of distribution of Cd(II) ions on the surface and pores of the adsorbent. Reports have it that when the numerical value of the constant, C equals q_{max} then adsorption is mainly a surface phenomenon but for smaller C value, the remaining adsorption could

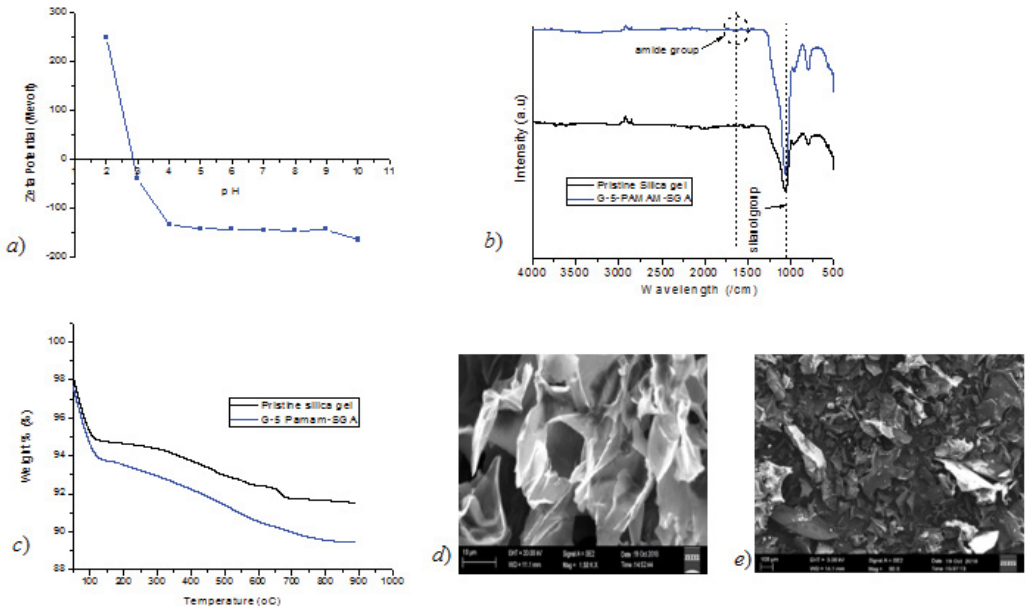

Figure 1: (a) Point of zero charge plot for G-5-PAMAM-SGA, (b) FTIR spectra of pristine silica gel and G-5-PAMAM-SGA, (c) TGA spectra of pristine silica gel and G-5-PAMAM-SGA, SEM micrograph of G-5-PAMAM-SGA, (d) Before Cd(II) adsorption and (e) After Cd(II) adsorption.

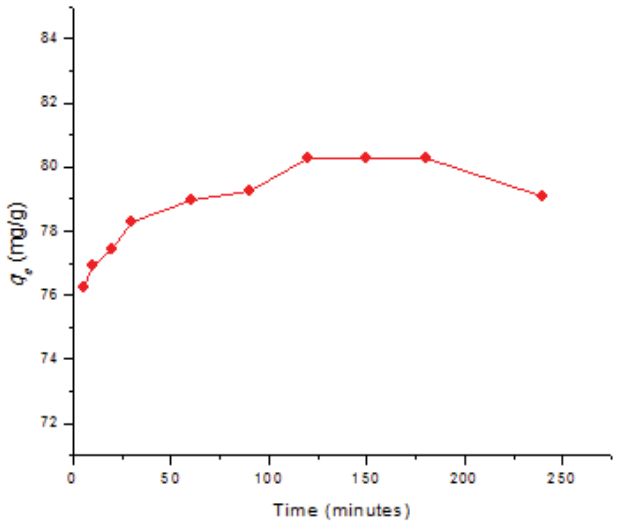

Figure 2: Adsorption trend for Cd(II) as time increased.

Model	Parameters
PFO	q_e (mg g^{-1})=7.360
	K_1 (min^{-1})=2.1 × 10^{-4}
	R^2=0.764
PSO	q_e (mg/g)=5.128
	K_2 (g mg^{-1} min^{-1})=2.535
	R^2=0.999
IPD	C (mg g^{-1})=86.934
	Kid (g g^{-1} min 1/2)=0.82799
	R2 = 0.5335
PPA	17.34
PSA	82.66
PPA: Proposed Pore Adsorption as predicted by IPD	
PSA: Proposed Surface Adsorption as predicted by IPD	

Table 1: Kinetic parameters for the adsorption of Cd (II) by G-5-PAMAM-SGA.

be attributed to pore filling [25]. As such the C value given in Table 1 reveals that approximately 82.66% was due to surface adsorption and 17.34% due to pore filling.

Effect of pH on Cd(II) uptake by G-5-PAMAM-SGA

Scientific investigations have shown that pH affects the charge density around adsorbate and adsorbent molecules [26]. Following the aforementioned the uptake of Cd(II) by G-5-PAMAM-SGA was investigated as pH was varied (Figure 3). The observed trend clarifies the effect of pH with respect to the point of zero charge of the adsorbent (2.9). Below the point of zero charge (2.9) the adsorbent becomes predominantly positively charged because of protonation of its surface-active functional groups, thus adsorption at this stage could be mainly due to pore filling. But with increase in pH value the surface of the adsorbent become negatively charged due to deprotonation and this facilitates electrostatic interactions between Cd(II) ions and the adsorbent. Therefore, higher adsorption values were observed as shown in Figure 3.

Effect of concentration and temperature on the uptake of Cd(II) ions by G-5-PAMAM-SGA

The trend showed an increase in Cd(II) adsorption by G-5-PAMAM-SGA as initial concentration (Co) increased from 75 through 175 mg/L. The drift was also observed at 20, 30 and 40°C respectively (Figure 4). This trend may be attributed to the activities of Cd(II) ions between the surface and the internal cavities of the adsorbent. At equilibrium, migration of Cd(II) ions between adsorbent surfaces and pores may be equal for specific concentration values (Co), therefore, movement of the ions across both boundaries would have been retarded. Nevertheless, increasing the concentration of the Cd(II) ions improved the migration of adsorbate molecules across both boundaries thus, there is an observed increase in adsorption [27].

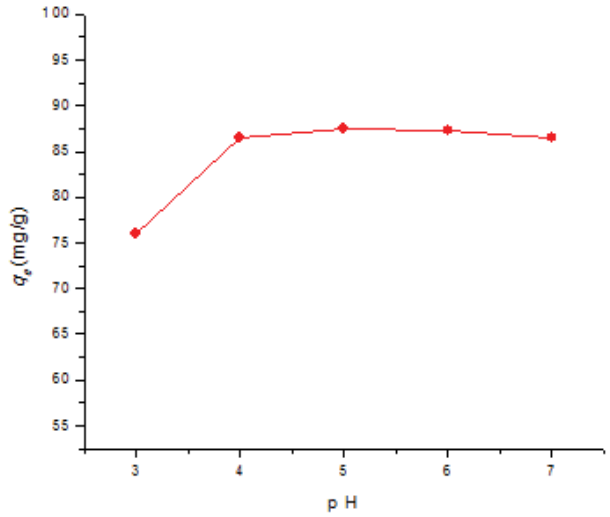

Figure 3: Effect of p^H on the uptake of Cd(II).

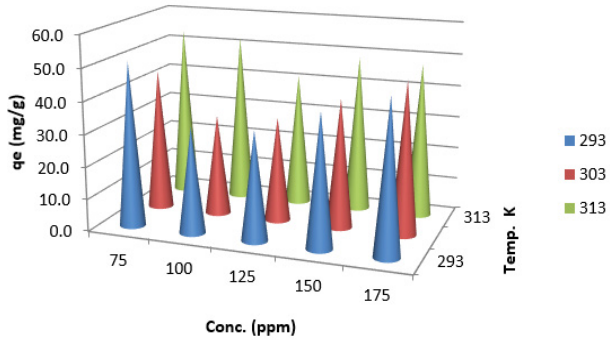

Figure 4: Effect of initial concentration and operating temperature on the uptake of Cd(II).

Equilibrium data at 293K were assessed using Langmuir, Freundlich, Harkins-Jura, Jossens, Sips and Baudu isotherm models, the isotherm parameters are shown in Table 2. Comparison of parameters of the models showed that experimental data fitted the Jossens more than the other models. Jossens model (r^2=0.981), Baudu (r^2=0.973), Harkins-Jura (r^2=0.9607), Sips (r^2 =0.953), Freundlich (r^2=0.952), and Langmuir (r^2=0.935). The good fitting of Jossens model with experimental data implies that the adsorbent has heterogeneous surface. Similarly, the high correlation coefficient obtained from Harkins-Jura model indicates that the adsorbent is heteroporous. Freundlich model also showed a good fit to experimental data with n>1, indicating chemisorption. Freundlich isotherm also showed good adsorption capacity (K_F=58.58) which suggests a multi-layered adsorption on a heterogeneous surface of unequal energy which is consistent with a previous report [28].

Increasing the ambient experimental temperature from 20 through 40°C showed that temperature had a positive effect on the adsorption of Cd(II) ions on G-5PAMAM-SGA; therefore, increasing the temperature, increases Cd(II) adsorption. This trend suggests an endothermic process for Cd(II) ions adsorption on the adsorbent. In order to determine this, the adsorption process was further examined using thermodynamic parameters(ΔH°, ΔS° and ΔG°) which were estimated from the experimental equilibrium data obtained at the various temperatures investigated and the parameters are shown in Table 3.

The ΔG° values for all temperatures studied were negative, this suggested spontaneous and feasible Cd(II) adsorption processes. The value of enthalpy change (ΔH°) was positive and this confirmed the supposition that the adsorption process was endothermic. In an endothermic process, any increase in external energy favors the forward process; consequently, Cd(II) adsorption improved with increase in solution temperature [29]. The positive value of the ΔS° is an indication of increased randomness of the Cd(II) ions in solution as the adsorption process progressed towards equilibrium. The calculated value for sticking probability (S^*) was approximately equal to 1, this signifies an adsorption mechanism having a combination of chemisorption and physisorption [30]. The low value of activation energy (Ea) is an indication of a diffusion-controlled sorption process [31-39].

Reusability and comparison with reported adsorbents

Desorption studies was carried out in order to appraise the economic prospects in the use of G-5-PAMAM-SGA as an adsorbent for the removal of Cd(II) ions from aqueous solutions. Results of three cycles reusability test using previously used G-5-PAMAM-SGA as adsorbent for Cd(II) removal is illustrated with Figure 5 it can be

Langmuir isotherm
q_{max} (mg/g)=20.33
b (L/mg)=7.49
$R_{L=}$0.001
R^2 =0.9352
Freundlich isotherm
K_F (mg/g)=58.57
1/n=0.2199
R^2=0.9525
Harkins-Jura isotherm
A (mg/g)=5000
B=-0.35
R^2=0.9607
Sips isotherm
K_S (L/g)=29.096
a_s (L/mol)
B_S=29.0846
R^2=0.9526
Jossens isotherm
q_{max} (mmol/g)=1.776
b_k (L/mmol)=195.191
a_k=-0.2990
R^2=0.9805
Baudu isotherm
q_{max} (mmol/g)=21.792
b_B (L/mmol)=8.2716
X=-0.3875
Y=0.6502
R^2=0.9726

Table 2: Adsorption isotherm models parameters for Cd (II).

Thermodynamics	Parameters	Cd (II)
ΔH°	kJ mol^{-1}	10.474
ΔS°	J mol^{-1} K^{-1}	11.399
ΔG° (kJ mol^{-1})	293 K	-3329.9
	303 K	-3443.27
	313 K	-3557.26
Ea (KJ mol^{-1})	3.3 × 10^{-3}	--
S^*	0.9999	--

Table 3: Thermodynamic parameters of G-5-PAMAM-SGA for Cd (II) adsorption.

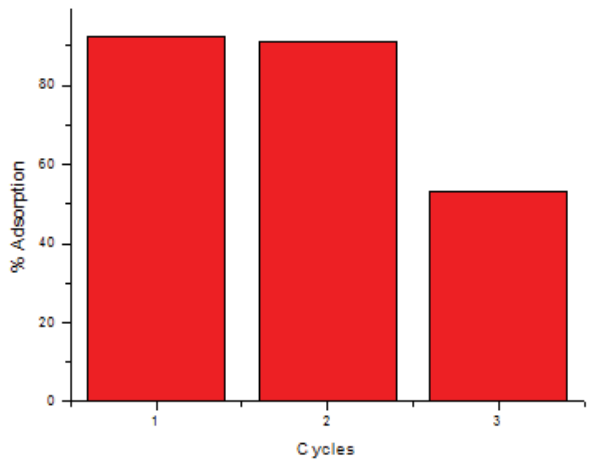

Figure 5 : Reusability chart showing three adsorption cycles.

Adsorbents	q_e (mg/g)	References
Hematite	4.94	32
Bentonite-*Carica papaya* composite	10.9	33
Feldspar-pine cone composite	11.5	34
Wheat stem	11.6	35
Chitin	14.7	36
BMF-0.5	15.8	37
Orange waste	48.3	38
G-5-PAMAM-SGA	123.4	This study
Biogenic Mn Oxide	229.3	39

Table 4: Comparison of G-5-PAMAM-SGA Cd (II) adsorption capacities of with those of some composites reported I literature.

deduced that the third cycle was slightly lower than the second cycle by approximately 35%.

The high adsorption exhibited in the first and second cycles could be due to availability of empty adsorption sites on the adsorbent. Meanwhile, desorption of Cd(II) ions during the first and second cycles was simple because the desorbing solvent could reach the surface adsorbed adsorbates easily, but adsorbates molecules that were initially adsorbed into adsorbent pores and crevices were not accessible at the third cycle of desorption. This led to a reduction in the removal capacity of the adsorbent by 35%.

The adsorption of Cd(II) ions by G-5-PAMA-SGA was compared with that of other adsorbents as shown in Table 4. The comparison revealed that G-5-PAMAM-SGA performed better that a number of adsorbents in the removal of Cd(II) ions. This serves as an indicator for the potentials of G-5-PAMAM-SGA as an effective adsorbent for the removal of Cd(II) ions from wastewater.

Conclusion

In this study G-5-PAMAM-Silica gel composite (G-5-PAMAM-SGA) was synthesized, characterized and used for the removal of Cd(II) ions from aqueous solution. Characterization results showed peaks of associated functional groups, larger pore size and slightly lower thermal stability when compared with unmodified silica gel. All proving a successful synthesis of G-5-PAMAM-SGA. SEM images revealed the presence of agglomerated Cd(II) ions on G-5-PAMAM-SGA. Equilibrium results showed that equilibrium was reached after 180 min, optimum pH=6 and q_{max}=123.4 mg/g which is better than that of several adsorbents in literature. Thermodynamic studies indicated endothermic, spontaneous and feasible adsorption process. The adsorption modelling parameters indicated multi-layered sorption onto heterogeneous/heteroporous adsorbent. Two processes were implicated in the sorption of Cd(II) ions by G-5-PAMAM-SGA namely; adsorptive pore filling of empty mesopores and electrostatic interactions between negatively charged surface groups and Cd(II) ions in solution.

Pseudo-second-order kinetic model described the adsorption process accurately thus, it was mainly controlled by chemisorption. Jossens, Harkins-Jura, and Freundlich models were the most reliable isotherm models for describing the sorption process as evidenced by high correlation coefficients. G-5-PAMAM-SGA exhibited good reusability after three cycles of desorption. These results imply that G-5-PAMAM-SGA could be efficient in the removal of Cd(II) ions from aqueous phases most especially during waste-water treatment procedures.

References

1. Ajmal M, Mohammad A, Yousuf R, Ahmad AC (1998) Adsorption behavior of Cadmium, Zinc, Nickel and Lead from aqueous solutions by MagniferaIndica seed shell India. J Environ Hith 40: 15-26.
2. Evanko CR, Dzombak DA (1997) Remediation of metals-contaminated soils and groundwater. Ground-Water Remediation Technologies Analysis Center, Pittsburg, USA.
3. Madu AN, Folawewo AD, Adebanjo MG (2017) Surface adsorption of some heavy metal ions in waste and underground waters in Agbara industrial estate using sodium metasilicate. IJSRCH 2: 22-29.
4. Sprynskyy M, Kosobucki P, Kowalkowski T, Buszewski B (2007) Influence of clinoptilolite rock on chemical speciation of selected heavy metals in sewage sludge. J Hazard Mater 149: 310-316.
5. Satarug S, Baker JR, Urbenjapol S, Haswell-Elkins M, Reilly PE, et al. (2003) A global perspective on cadmium pollution and toxicity in non-occupationally exposed population. Toxicology Letters 137: 65-83.
6. GESAMP (1987) /IMO/FAD/UNESCO/WMO/WHO/IAEA/UN/UNEP. Joint group of experts on the scientific aspects of marine pollution: Report of the seventeenth session, reports an studies, 31: 172.
7. Wilson DN (1988) Cadmium–market trends and influences. In Cadmium 87. Proceedings of the 6th International Cadmium Conference, London, Cadmium Association 9: 16.
8. McLaughlin MJ, Singh BR (1999) Cadmium in soils and plants. In Cadmium in Soils and Plants, Springer, Dordrecht, pp: 1-9.
9. Stohs SJ, Bagchi D (1995) Oxidative mechanisms in the toxicity of metal ions. Free Radical Biology and Medicine 18: 321-336.
10. Mitra RS (1984) Protein synthesis in Escherichia coli during recovery from exposure to low levels of Cd2+. Appl Environ Microbiol 47: 1012-1016.
11. McCluggage D (1991) Heavy metal Oisoning. NCS Magazine, The Bed Hospital. Co.u.s.a (HYPERLINK "http://www.cocicaties.org/articles/diseases/metals.html" www.cocicaties.org/articles/diseases/metals.html)
12. Qu R, Wang M, Sun C, Zhang Y, Ji C, et al. (2008) Chemical modification of silica-gel with hydroxyl-or amino-terminated polyamine for adsorption of Au (III). Applied Surface Science 255: 3361-3370.
13. Hughes MA, Wood J, Rosenberg E (2008) Polymer structure and metal ion selectivity in silica polyamine composites modified with sodium chloroacetate and nitriloacetic acid (NTA) anhydride. Industrial & Engineering Chemistry Research 47: 6765-6774.
14. Gunatilake SK (2015) Methods of removing heavy metals from industrial wastewater. Methods 1: 14.
15. Kazeem TS, Lateef SA, Ganiyu SA, Qamaruddin M, Tanimu A, et al. (2018) Aluminium-modified activated carbon as efficient adsorbent for cleaning of cationic dye in wastewater. Journal of Cleaner Production 205: 303-312.
16. Acres RG, Ellis AV, Alvino J, Lenahan CE, Khodakov DA, et al. (2012) Molecular structure of 3-aminopropyltriethoxysilane layers formed on silanol-terminated silicon surfaces. The Journal of Physical Chemistry C 116: 6289-6297.

17. Shi X, Sun K, Balogh LP, Baker JJR (2006) Synthesis, characterization, and manipulation of dendrimer-stabilized iron sulfide nanoparticles. Nanotechnology 17: 4554.

18. Jiang Y, Gao Q, Yu H, Chen Y, Deng F (2007) Intensively competitive adsorption for heavy metal ions by PAMAM-SBA-15 and EDTA-PAMAM-SBA-15 inorganic–organic hybrid materials. Microporous and Mesoporous Materials, 103: 316-324.

19. Emeka-Okorie HOC, Ekemeie PN, Akpomie KG, Olikagu CS (2018) Frontiers in Chemistry, 6.

20. Lagergren S (1898) Zur theorie der sogenannten adsorption geloster stoffe. Kungliga svenska vetenskapsakademiens. Handlingar 24: 1-39.

21. Weber WJ, Morris JC, Sanit J (1963) Engineering Division. Am Soc Civil Eng 89: 31-60.

22. Ayawei N, Ebelegi NA, Wankasi D (2017) Modelling and Interpretation of Adsorption Isotherms. Hindawi Journal of Chemistry, doi. org/10.1155/2017/3039817

23. Abasi CY, Diagboya PNE, Dikio ED (2019) Synthesis, characterisation of ternary layered double hydroxides (LDH) for sorption kinetics and thermodynamics of Cd^{2+}. International Journal of Environmental Studies pp: 1-15.

24. Boparai HK, Joseph M, O'Carroll DM (2011) Kinetics and thermodynamics of cadmium ion removal by adsorption onto nano zerovalent iron particles. J Hazard Mater 186: 458-465.

25. Repo E, Warchoł JK, Bhatnagar A, Sillanpää M (2011) Heavy metals adsorption by novel EDTA-modified chitosan–silica hybrid materials. Journal of Colloid and Interface Science 358: 261-267.

26. Diagboya PN, Olu-Owolabi BI, Adebowale KO (2014) Microscale scavenging of pentachlorophenol in water using amine and tripolyphosphate-grafted SBA-15 silica: Batch and modeling studies. Journal of Environmental Management 146: 42-49.

27. Asuquo ED, Martin AD (2016) Sorption of cadmium (II) ion from aqueous solution onto sweet potato (*Ipomoea batatas* L.) peel adsorbent: characterisation, kinetic and isotherm studies. Journal of Environmental Chemical Engineering 4: 4207-4228.

28. Sharma YC (2008) Thermodynamics of removal of cadmium by adsorption on an indigenous clay. Chemical Engineering Journal 145: 64-68.

29. Ajmal M, Mohammad A, Yousuf R, Ahmad AC (1998) Adsorption behavior of Cadmium, Zinc, Nickel and Lead from aqueous solutions by MagniferaIndica seed shell India. J Environ Hith 40: 15-26.

30. Wankasi D (2013) Asorption: A guide to experimental analysis. Amplitude Printing Soluions, Portharcourt, Nigeria. pp. 42.

31. Olu-Owolabi BI, Alabi AH, Unuabonah EI, Diagboya PN, Böhm L, et al. (2016) Calcined biomass-modified bentonite clay for removal of aqueous metal ions. J Environ Chem Eng 4: 1376-1382.

32. Singh DB, Rupainwar DC, Prasad G, Jayaprakas KC (1998) Studies on the Cd (II) removal from water by adsorption. J Hazard Mater 60: 29-40.

33. Olu-Owolabi BI, Diagboya PN, Unuabonah EI, Alabi AH, Duering RA, et al. (2018) Fractal-like concepts for evaluation of toxic metals adsorption efficiency of feldspar-biomass composites. J Clean Prod 171: 884-891.

34. Tan G, Xiao D (2009) Adsorption of cadmium ion from aqueous solution by ground wheat stems. J Hazard Mater 164: 1359-1363.

35. Benguella B, Benaissa H (2002) Cadmium removal from aqueous solutions by chitin: Kinetic and equilibrium studies. Water Research 36: 2463-2474.

36. Diagboya PN, Dikio ED (2018) Scavenging of aqueous toxic organic and inorganic cations using novel facile magneto-carbon black-clay composite adsorbent. J Clean Prod 180: 71-80.

37. Pérez-Marín AB, Zapata VM, Ortuno JF, Aguilar M, Sáez J, et al. (2007) Removal of cadmium from aqueous solutions by adsorption onto orange waste. J Hazard Mater 139: 122-131.

38. Soltani RDC, Jafari AJ, Khorramabadi GS (2009) Investigation of cadmium (II) ions biosorption onto pretreated dried activated sludge. American Journal of Environmental Sciences 5: 41.

39. Meng YT, Zheng YM, Zhang LM, He JZ (2009) Biogenic Mn oxides for effective adsorption of Cd from aquatic environment. Environmental Pollution 157: 2577-2583.